Available online at www.sciencedirect.com
ScienceDirect
Journal of Nuclear Materials 358 (2006) 151–163
journal of nuclear materials
www.elsevier.com/locate/jnucmat

Tungsten bronze-based nuclear waste form ceramics. Part 2: Conversion of granular microporous tungstate–polyacrylonitrile (PAN) composite adsorbents to leach resistant ceramics

Christopher S. Griffith [a], Ferdinand Sebesta [b], John V. Hanna [a], Patrick Yee [a], Elizabeth Drabarek [a], Mark E. Smith [c], Vittorio Luca [a,*]

[a] *Australian Nuclear Science and Technology Organisation, Institute of Materials and Engineering Sciences, PMB 1, Menai, NSW 2234, Australia*
[b] *Czech Technical University in Prague, Department of Nuclear Chemistry, Břehová 7, 115 19 Prague 1, Czech Republic*
[c] *Department of Physics, University of Warwick, Gibbett Hill Road, Coventry CV47AL, UK*

Received 17 January 2006; accepted 26 June 2006

Abstract

Conversion of a granular molybdenum-doped, hexagonal tungsten bronze (MoW–HTB)–polyacrylonitrile (PAN) composite adsorbent to a leach resistant ceramic waste form capable of immobilizing adsorbed Cs^+ and Sr^{2+} has been achieved by heating in air at temperatures in the range 600–1200 °C. Thermal treatment of the Cs- and Sr-loaded composite material at 1000 °C was sufficient to invoke a 60% reduction in volume of the composite while still retaining its spherical morphology. Cs-133 MAS NMR studies of this sample suite at 9.4 T and 14.1 T showed that multiple Cs sites are present throughout the entire thermal treatment range. Scanning electron microscopy investigations of the phase assemblages resulting from thermal treatment demonstrated that the full complement of Cs, and the majority of Sr, partitions into HTB phases ($A_{0.16–0.3}MO_3$; A = Cs^+, Sr^{2+} and Na^+; M = Mo, W). The potentially reducing conditions resulting from the removal of the PAN matrix or the presence of high concentrations of Na^+ relative to either Cs^+ or Sr^{2+} does not retard the formation of the high temperature HTB phases. The fraction of Cs^+ and Sr^{2+} leached from the tungstate phase assemblages was superior or comparable with cesium hollandite ($Cs_{0.8}Ba_{0.4}Ti_8O_{18}$; $f = \approx 8 \times 10^{-5}$; rate = $<1.2 \times 10^{-4}$ g/m^2/day) and strontium titanate ($SrTiO_3$; $f = 3.1 \times 10^{-3}$; rate = 2.63×10^{-4} g/m^2/day), respectively, using a modified PCT test in Millipore water at 90 °C. Furthermore, where aggressive leaching conditions were employed (0.1 M HNO_3; 150 °C; 4 days), the tungstate phase assemblages displayed leach resistance almost two orders of magnitude greater than the reference phases.

1. Introduction

Recent work by our group has demonstrated that fine grained hexagonal tungsten bronze (HTB) materials prepared through hydrothermal methods

* Corresponding author.
E-mail address: vlu@ansto.gov.au (V. Luca).

0022-3115/$ - see front matter
doi:10.1016/j.jnucmat.2006.06.018

show useful selectivity for the separation of Cs^+ and Sr^{2+} from acidic solutions [1]. This preliminary study was followed by a detailed characterization of the ion exchange properties of the Mo-doped phase [2]. Following on from this we have demonstrated that such compounds can potentially be converted into leach resistant ceramics [3]. In part 1 of this series we provided a comprehensive evaluation of the leach resistance of the bronze materials generated by heat treatment of Cs-, Sr- and lanthanide-loaded HTB ion exchange materials and a more complete description of the phase chemistry of the HTB waste form system. The conversion of a saturated adsorbent into a leach resistant ceramic has been termed the 'cradle-to-grave' approach in which separation and immobilization are carried out on the same chemical system. This strategy has many attractive aspects for nuclear waste management including waste volume reduction and simplification of processing since there is no need to undertake combination of a liquid radioactive feed stream with oxide components.

While fine grained powders and batch mode processing can in principle be used to effect ion exchange separations, large scale industrial treatment of a waste stream is more likely to require granular materials. However, engineering of granular materials from ion exchange materials can be difficult and usually results in a degradation of their ion exchange properties. One option for granulation is to incorporate, or support, the active inorganic adsorbent phase on a polymer matrix. Sebesta and colleagues have pioneered the development of a universal support based on polyacrylonitrile (PAN) [4,5] with others also employing this strategy. We too have used this strategy to produce HTB–PAN composites suitable for deployment in a column and have fully characterized the ion exchange performance of such composites in columns using simulated [6] and actual intermediate level liquid waste streams. The HTB–PAN composites display comparable ion exchange kinetics and capacity to the parent microporous adsorbent. Since the reason for interest in inorganic ion exchange materials in the first place is due to their high selectivity and radiation stability it might seem contradictory to resort to the use of a polymer support matrix. However, it needs to be appreciated that in the case of the HTB–PAN composite, the PAN component acts only as a support, the only requirement of which is to maintain its mechanical integrity during use. The use of PAN was seen by us as a convenient means of producing granular materials for column evaluations. The present contribution to this series is dedicated to determining the performance of waste form materials derived from the HTB–PAN ion exchanger composite. Two major issues with this approach are whether the tungstate phase chemistry will be significantly influenced by the more reducing conditions resulting from the removal of the PAN matrix, and/or the lower level of adsorbed cesium and strontium in comparison to that employed during part 1 of this series. The leaching behavior of the phase assemblages formed from calcination of this material between 600 and 1200 °C, in Millipore water at 90 °C (1, 4 and 7 days) and 0.1 M HNO_3 at 150 °C (4 days) will be presented. We will describe the thermal treatment of HTB–PAN composite adsorber with composition, $Cs_{0.063}Sr_{0.058}Mo_{0.03}W_{0.97}O_3 \cdot ZH_2O$-polyacrylonitrile (CsSr–MoW–HTB–PAN), which is indicative of the low Cs- and Sr-loading arising from fixed-bed column separation of Cs^+ and Sr^{2+} from acidic radwaste stimulant.

2. Experimental

As in part 1 all chemicals utilised were supplied by Aldrich or Fluka and were of analytical grade unless otherwise stated. The instrumentation used to characterized the parent $Na_{0.3}Mo_{0.03}W_{0.97}O_3 \cdot Z(H_2O)$ (MoW–HTB) absorbent and calcined CsSr–MoW–HTB–PAN materials was the same as in part 1.

2.1. Synthesis of CsSr–MoW–HTB–PAN and CsSr–MoW–HTB–PAN-x (x = 600, 800, 1000 and 1200 °C)

The microporous, tungsten oxide-based adsorbent, $Na_{0.2}Mo_{0.03}W_{0.97}O_3 \cdot Z(H_2O)$ (MoW–HTB), was prepared *via* a modification of the procedure outlined by Reis and co-workers [7]. The MoW–HTB–PAN composite absorber (60% w/w) was prepared via the method described previously [8]. The material was supplied as air-dried beads (<0.8 mm diameter) with the percentage weight loading of the inorganic adsorbent determined by simultaneous TG/DT analysis and subsequent monitoring of the PAN matrix removal upon heating to ~500 °C. Cesium- and strontium-loading of the MoW–HTB–PAN composite was conducted using an acidic solution of Cs^+ (51 ppm) and Sr^{2+} (31 ppm) (500 ml) for 24 h under agitation. On the

basis of the initial and final concentrations of Cs^+ and Sr^{2+} in solution as determined by ICPMS the individual uptake levels were calculated. Samples of CsSr–MoW–HTB–PAN-*x* ($x = 600$, 800, 1000 and 1200 °C) were prepared by pelletising CsSr–MoW–HTB–PAN (2.0 g) using a 15 mm die (1 tonne). The resultant pellet was then calcined in a platinum crucible in air, at either 600, 800, 1000, 1200 or 1300 °C (*x*) (heating profile: 10 °C min^{-1}/*x* °C/300 min/−10 °C min^{-1}/30 °C).

2.2. Leaching studies of CsSrMoHTB–PAN-x (x = 600, 800, 1000 and 1200 °C)

Samples of the calcined CsSr–MoW–HTB–PAN-*x* pellets were ground and the 30–50 μm size fraction of each isolated using a Gilson ultrasonic sieve apparatus. An unwashed portion of each (~100 mg) was introduced into a Teflon jar (Savillex) along with Millipore water (10 ml) to give a volume-to-mass ratio of 100 ml/g. All experiments were conducted in duplicate. The containers were sealed and heated (90 ± 1 °C) for 1, 4 or 7 days. After the appropriate time the supernatant from each leach test was removed, filtered (0.2 μm) and immediately acidified with ultra-pure HNO_3 to minimise precipitation of any dissolved elements prior to analysis by ICPMS. The fraction of Cs^+ or Sr^{2+} leached (*f*) for given time periods and normalized cation release rates (g/m^2/day) were determined as per in part 1. More aggressive leach tests were conducted with similar materials and 0.1 M HNO_3 at 150 °C in Teflon lined hydrothermal reaction vessels (45 ml) for 4 days at a volume-to-mass ratio of 100 ml/g.

2.3. Magic-angle-spinning NMR

High resolution ^{133}Cs magic-angle-spinning (MAS) NMR studies were undertaken at ambient temperatures on a Bruker MSL-400 (9.4 T) and Chemagnetics CMX-600 (14.1 T) spectrometers operating at ^{133}Cs frequencies of 52.5 MHz and 76.0 MHz, respectively. At 9.4 T, all data were acquired using a Bruker 4 mm MAS probe in which MAS frequencies of 15 kHz were implemented. All 14.1 T data was acquired with a 4 mm Varian-Chemagnetics T3 MAS probe in which MAS frequencies of up to 20 kHz were achieved. At these magnetic field strengths, all pulse conditions were calibrated on a 1 M CsCl solution from which a 'non-selective' π/2 pulse time of 6 μs was measured. This corresponded to a 'selective' π/2 pulse time for the spin-7/2 ^{133}Cs nucleus of 2 μs. From this calibration, a π/4 pulse time of 1 μs and a recycle delay of 3 s were used for all measurements. This 1 M CsCl solution was also used as a chemical shift reference at each field thus representing 0.0 ppm.

The elemental ratios in the composite adsorbent were determined by X-ray fluorescence (XRF) analysis using a wavelength dispersive Philips PW2400 X-ray fluorescence spectrometer equipped with a rhodium anode tube. Samples were prepared by pressing in boric acid. All the samples were fused with a sample-to-flux ratio of 1–8. The fusion temperature was 1050 °C. The flux used was 12:22 lithium tetraborate to lithium metaborate. The Uniquant program suite was used for analysis of all data.

3. Results

3.1. Cesium and strontium-loading of MoW–HTB–PAN composite adsorber

The static batch contact of MoW–HTB–PAN composite adsorbent with an acidic solution containing Cs^+ and Sr^{2+} afforded material of nominal composition, $Cs_{0.063}Sr_{0.058}$MoW–HTB–PAN (CsSr–MoW–HTB–PAN). Our previous work on the fixed-bed column performance of the MoW–HTB–PAN composite adsorbent and acidic ANSTO legacy radwaste stimulant has shown that the composition of the exhausted composite approaches $Cs_{0.08}Sr_{0.005}$–MoW–HTB–PAN [6]. In the present study a higher level of Sr was employed in order to aid identification of Sr-containing phases. Importantly the levels of Cs and Sr are still significantly less than that studied in part 1 of this series, and so are far more representative of an exhausted adsorbent for disposal. Previous investigations have also demonstrated that the theoretical capacity of the parent adsorbent MoW–HTB phase is never achieved as a proportion of the Na^+ initially present in the MoW–HTB phase is not exchangeable even under the acidic loading conditions, or through exchange with Cs^+ or Sr^{2+} [2]. XRF analysis of the CsSr–MoW–HTB–PAN composite confirmed the levels of Cs and Sr calculated from the ICP-MS analysis, as well as indicating the level of Na remaining in the inorganic adsorbent so that a nominal composition of $Na_{0.054}Cs_{0.063}$-$Sr_{0.058}$–MoW–HTB–PAN was determined for the exhausted adsorbent surrogate. These Cs and Sr

loadings are far less than those studied in part 1 of this series.

3.2. Thermal transformation of CsSr–MoW–HTB–PAN adsorbent

A plot of the thermogravimetric analysis and differential thermal analysis of CsSr–MoW–HTB–PAN is shown in Fig. 1. The major features of the thermal analysis are two exotherms at 315 and 509 °C. The lower temperature exotherm probably represents both the removal of physisorbed water on the surfaces of the MoW–HTB particles and within the structural channels, and partial decomposition of the PAN matrix while the higher temperature exotherm is due to complete combustion of the organic component. The final stages of the PAN matrix removal masks an exotherm routinely observed at 500 °C which is characteristic of the decomposition of the HTB framework and the crystallization of WO_3 [2,3]. The region between the end of this decomposition and 1200 °C shows minimal weight loss from the sample but between 1200 and 1300 °C there was mass loss of approximately 5% from the sample. This is in accord with our previous studies on cesium volatilization in the HTB system [3]. Two weak endotherms were observed at 1250 °C that are attributable to two melt transitions based on their asymmetric lineshape (Fig. 1 inset).

The macroscopic changes to the CsSr–MoW–HTB–PAN beads upon thermal treatment between 600 and 1200 °C are clearly evident from the images presented in Fig. 2(a)–(d). The corresponding surface area (m^2/g) measurements and estimated percentage volume reduction (relative to CsSr–MoW–HTB–PAN) are given in Table 1. Removal

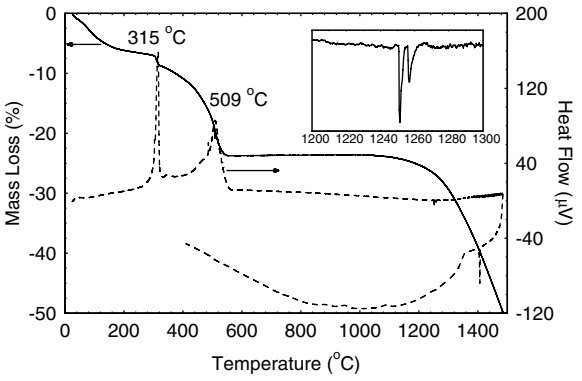

Fig. 1. TGA (—) and differential TGA (- - -) plot for CsSr–MoW–HTB–PAN composite adsorbent (30–1500 °C). Inset: Expansion of the high temperature regime.

of the organic PAN matrix on heating to 600 °C does not dramatically alter the size and appearance relative to the parent composite. However, the robustness of this material was significantly impacted with fragmentation of the granules occurring on extended manipulation. On heating to between 800 and 1000 °C, the volume of the individual adsorbent particles decreased between 40% and 60% and the granules were significantly more robust. As supported by the thermal analysis, partial melting of the resultant tungstate assemblage was observed at 1200 °C (Fig. 2(d)) with complete melting observed at 1300 °C (not shown in Fig. 2). The surface area of the CsSr–MoW–HTB–PAN-x materials ($x = 800$–1200 °C) were substantially less than that of the unheated native CsSr–MoW–HTB–PAN (0.6–0.8 m^2/g compared with 2.2 m^2/g). We are yet to explore hot isostatic pressing (HIPing) as a means to produce fully dense variants at elevated temperatures. However, the 1200 °C heated material is estimated to be close to full density since this material is composed of very large single crystals which are themselves fully dense.

In our previous work concerning the ion exchange properties of hexagonal tungsten bronze phases and Mo-doped variants, we reported that the MoW–HTB ion-exchanger is a monophasic material consisting of micron and sub-micron particles [1,2]. The XRD pattern (Fig. 3(a)) of this phase is typical of a poorly crystalline material containing significant disorder. The XRD patterns of composite materials heated between 600 and 1200 °C (Fig. 3(b)–(e)) demonstrates the presence of substantial proportions of monoclinic ($P2_1/n$) WO_3 as judged by the characteristic triplet of reflections centred around 23°2θ and other major reflections. The intensities of reflections attributed to the WO_3 phase differ very slightly from that expected for pure WO_3 and this seems entirely reasonable given that the results of the SEM investigations (below) confirm the incorporation of varying degrees of molybdenum in the principal WO_3-like phase at each calcination temperature. A degree of preferred orientation in the samples also cannot be discounted. For MoW–HTB samples which had been saturated with Cs^+ and/or Sr^{2+} the resultant XRD patterns in the angular range 5–25°2θ clearly demonstrated the presence of phases other than monoclinic WO_3 [3], but in the case at hand, where the concentrations of Cs^+ and Sr^{2+} were significantly lower, the presence of such phases was less obvious (Fig. 4(b)–(e)). The number and intensity of reflections

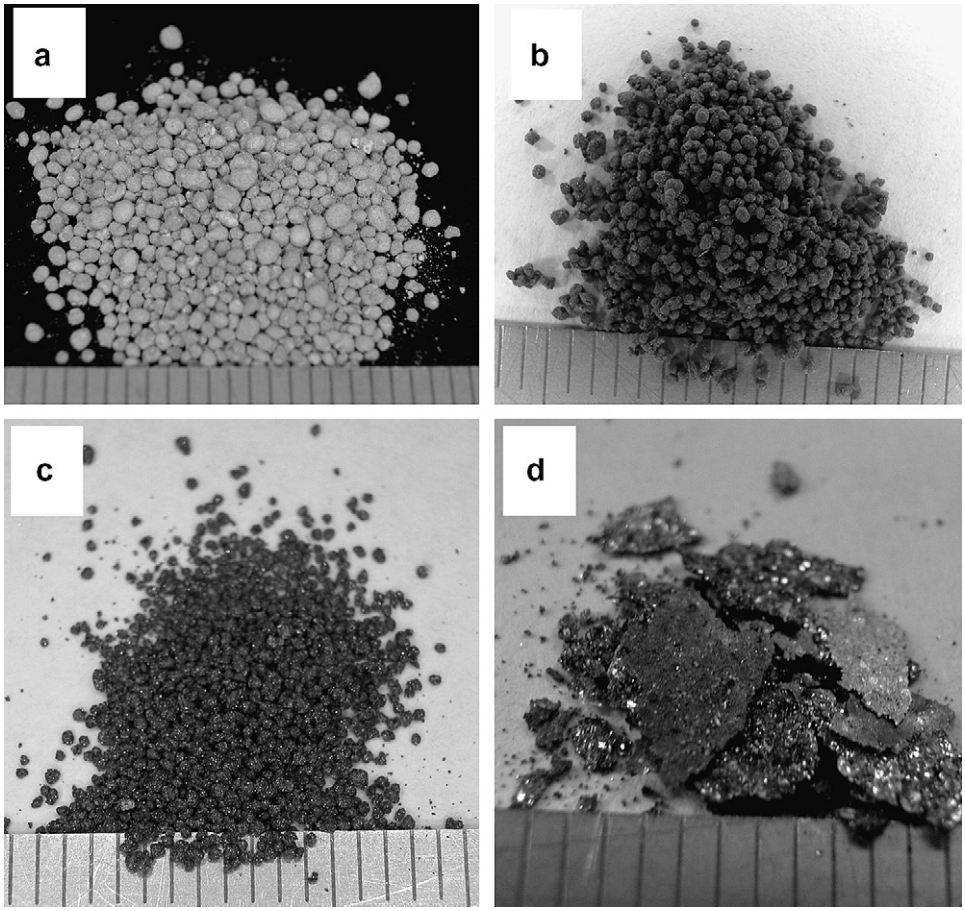

Fig. 2. Photographs of CsSr–MoW–HTB–PAN granular composite adsorbents after calcination at (a) 600, (b), 800, (c) 1000 and (d) 1200 °C. Graduations = 1 mm.

Table 1
Selected physical properties for CsSr–MoW–HTB-x (x = 600, 800, 1000 and 1200)

x	S_{BET} (m^2/g)	Estimated vol. reduction (%)
600	2.17	<5
800	0.63	40–50
1000	0.79	50–60
1200	0.83	nd

from the ancillary phases present in each sample have hampered direct efforts to assign each of the cation-containing phases; however, reflections at 14.5°2θ in each sample are indicative of a HTB-like phase. The fact that there were a number of such reflections indicates that there could be multiple HTB phases. Moreover, the series of harmonic reflections observed at very low angles provides evidence for intergrowth HTB–WO_3 structures as was suggested in part 1. From the back-scattered electron micrographs of the calcined samples (Fig. 6–9) the particle size of phases with compositions typical of the HTB phase ($A_{0.2–0.3}MO_3$) are >1 μm, and hence the broadened lineshape of the principal low angle HTB reflection is not likely to be due to particle size effects. The varying position and FWHM of this reflection does tend to indicate that the HTB-like phases present have varying unit cell parameters and/or compositional variations.

The 9.4 T ^{133}Cs MAS NMR spectra of the sample dried at 70 °C and samples heated to various temperatures are shown in Fig. 5(A) and generally consist of complex lineshapes. Such lineshapes may arise from multiple species and/or second order quadrupole interactions. In order to exclude the second of these possibilities we also recorded spectra at the higher field of 14.1 T. These spectra were very similar to those obtained at the lower field and so it is clear that multiple Cs species are present at all temperatures. Spectral decomposition using a minimum number of mixed Gaussian–Loretzian

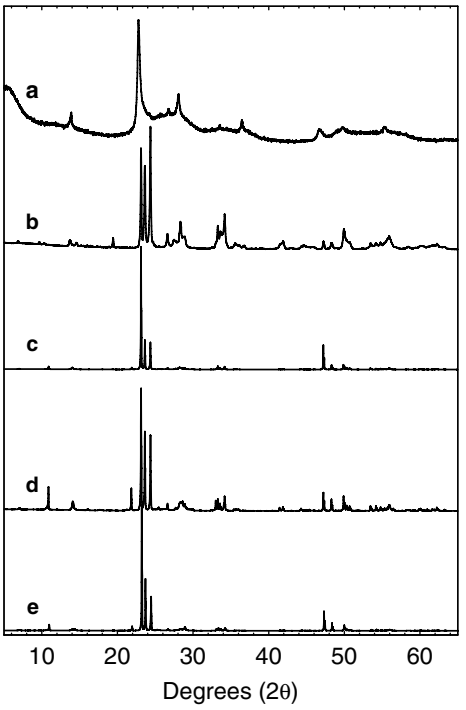

Fig. 3. XRD patterns (5–65°2θ) of CsSr–MoW–HTB–PAN composite absorber (a) before and after calcination in air at (b) 600, (c) 800, (d) 1000 and (e) 1200 °C.

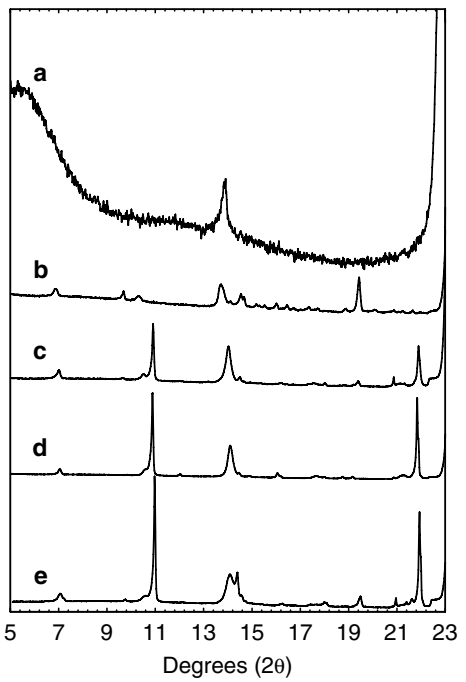

Fig. 4. XRD patterns (5–22.5°2θ) of CsSr–MoW–HTB–PAN composite absorber (a) before and after calcination in air at (b) 600, (c) 800, (d) 1000 and (e) 1200 °C.

lineshapes indicated that in all spectra at least three Cs species were present. While in crystallographic terms the HTB structure possesses only one site in which Cs can reside there are a number of possible explanations for the existence of multiple resonances. For example, variability in water coordination within the tunnels, Cs binding to surface sites, and compositional variations. While the air-dried sample contained water, heating to 600 °C was sufficient to drive water out of the structure irreversibly. Yet this spectrum was remarkably similar to that of the sample dried at 70 °C. This implies that

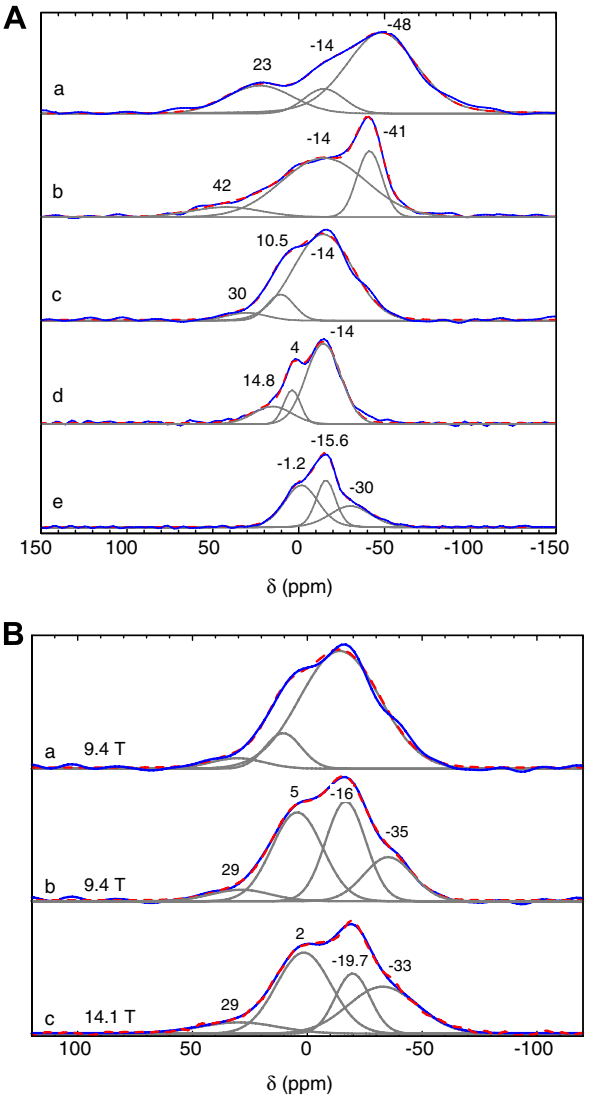

Fig. 5. (A) 9.4 T ^{133}Cs MAS NMR spectra for CsSr–MoW–HTB–PAN phase assemblages heated at (a) 70, (b) 600, (c) 800 (d) 1000 and (e) 1200 °C. (B) Comparison of (a) 3- and (b) 4-peak fitting models for 9.4 T data with (c) 14.1 T data.

Cs site variability is not due to water but more likely from variations in composition and structure. In other words, the samples contain a range of similar but slightly different Cs-containing phases.

The NMR spectrum of the CsSr–MoW–HTB–PAN-800 displayed three distinct Cs species but was noticeably different to that of the preceding sample in having a much narrower range of chemical shifts. Close inspection of this spectrum also revealed that the 3-peak model was a relatively poorer fit to this data than it was to the data of samples heated to all other temperatures. In particular a shoulder was observed on the low frequency (upfield) side of the spectral envelope at about −35 ppm. This shoulder was also present in the 14.1 T data which was fitted using a 4-peak model (Fig. 5(Bc)). This confirms that there is a progressive downfield shift of this resonance on heating from 70 (−48 ppm) to 800 °C (−35 ppm). Heating to 1000 °C resulted in little change to the spectrum except for a further narrowing of the range of the three chemical shifts observed. In the spectrum of the CsSr–MoW–HTB–PAN-1200 sample, a further significant change occurred in which a high field resonance was once again apparent at about −30 ppm.

Previous TEM investigations of unheated, Cs-saturated MoW–HTB samples have shown three distinct particle morphologies with similar Mo contents but quite different Cs contents. The Cs content of fine grained shards and fibres was found to be consistently higher than that of larger particles with a plate morphology [2]. Like the TEM of the unheated, Cs-saturated material, and in agreement with the XRD patterns, the cross-sectional SEM of the CsSr–MoW–HTB–PAN-600 sample confirmed the sample to be a multiphase assemblage (Fig. 6). Since the EDS lines of Sr and W overlap, quantification of Sr is less certain than it is for Cs. Because of this, and relatively significant spot-to-spot variability in the Cs and Sr analyses, we prefer here to give a total range for the Cs and Sr element ratios expressed as simply 'A' in the formula for particular morphologies. Large fibrous particles (region 1) are likely to be HTB material with an approximate composition $A_{0.16–0.25}Mo_{0.1}W_{0.9}O_3$. Importantly, these phases each contained an essentially comparable amount of Na and Cs. Ill-defined regions adjacent to the rod-like HTB fibres (region 2) contained high concentrations of Na in addition to comparable concentrations of both Sr and Cs to the large fibrous particles but an Mo content that was about 50% higher than in the rod-like HTB

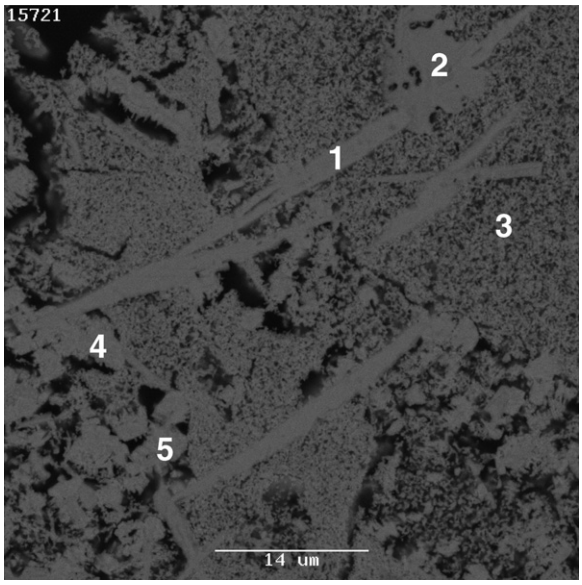

Fig. 6. SEM micrograph of CsSr–MoW–HTB–PAN-600. Spot EDS analyses were taken at the center of the marks. 1 – $A_{0.16–0.25}Mo_{0.1}W_{0.9}O_3$; 2 – $A_{0.24}Mo_{0.15–0.18}W_{0.82–0.85}O_3$; 3 – $A_{<0.06}Mo_{0.06–0.1}W_{0.9–0.94}O_3$; 4 – $A_{<0.06}Mo_{0.06–0.1}W_{0.9–0.94}O_3$; 5 – $A_{<0.06}Mo_{0.06–0.1}W_{0.9–0.94}$.

crystallites. This suggests that some degree of molybdenum partitioning occurs even at low calcination temperatures. On the basis of other evidence to be provided in the third part of this series, we have also assigned this composition to a bronzoid phase. The formation of substantial quantities of a WO_3-like phase (small crystallites; regions 3–5 of Fig. 6) having a typical composition of $A_{<0.06}MO_3$ (A = Na, Cs, Sr; M = Mo, W)) was clearly evident. Additionally, densification of the MO_3 regions was minimal and the level of molybdenum incorporation was consistently observed to be between 6% and 10% of the total metal content. These SEM observations are very much consistent with the NMR data for the CsSr–MoW–HTB–PAN-600 sample which also provided evidence for three discrete Cs-containing phases. We have therefore tentatively assigned the narrow resonance with a chemical shift of −41.4 ppm to the large fibrous crystallites (phase 1) with the lower Cs content since dipolar broadening and inhomogenous broadening should be less than that for the high abundance, high Cs- and Mo-content, and less crystalline Phase 2 material which is probably responsible for the chemical shift at −14.4 ppm. The low intensity resonance at 41.8 ppm might therefore be due to the very fine grained WO_3 particles with very small concentrations of both Cs and Mo.

The cross-sectional SEM image of the CsSr–MoW–HTB–PAN-800 sample is shown in Fig. 7 and was similar to that of the CsSr–MoW–HTB–PAN-600 sample. Clear densification occurred on increasing the calcination temperature from 600 to 800 °C. Regular shaped 100 μm blocks comprised the majority of this sample and analysed almost exclusively as $Mo_{0.02}W_{0.98}O_3$ (region 2). This composition and the number of such crystallites throughout the sample might suggest that regions of substantially increased molybdenum content should have been observed within the phase assemblage but we were unable locate any such phases. Furthermore, there was no evidence of MoO_3 or cesium molybdate phases from the corresponding XRD patterns. The interstitial regions between the $Mo_{0.02}W_{0.98}O_3$ crystallites consisted of well defined rod-like crystallites (region 1 and 3) and ill-defined regions that exhibited varying degrees of striation (4 and 5). At the resolution of the SEM employed, it is unclear whether these striated regions consist of extremely small crystallites or fused rod-shaped crystallites. The majority of the rod-like crystallites observed were typically between 2 and 4 μm thick and up to 20 μm in length. The larger of these rod-like crystallites contained equal proportions of Cs and Na as was observed for the CsSr–MoW–HTB–PAN-600 sample but importantly contained no Sr. The smaller crystallites were of similar composition but appeared to contain some Sr, although the level was almost on the limit of detection using the EDS technique. This clearly indicates that heating to 800 °C results in some degree of Sr partitioning away from the Cs-containing HTB phases. The majority of Sr was found in the interstitial regions in phases which analysed as $A_{0.35-0.4}Mo_{0.02}W_{0.98}O_3$. These regions were generally very rich in Na and possessed a stoichiometry which was at the limit typical for the HTB phase ($A_{0.3}MO_3$). Thus in this sample also, there is direct evidence for at least two different Cs-containing phases.

Fig. 7. SEM micrograph of CsSr–MoW–HTB–PAN-800. Spot EDS analyses were taken at the centre of the marks. 1 – $A_{0.35}WO_3$; 2 – $A_{<0.06}Mo_{0.02}W_{0.98}O_3$; 3 – $A_{0.26}WO_3$; 4 – $A_{0.4}Mo_{0.02}W_{0.98}O_3$; 5 – $A_{0.35-0.38}Mo_{0.02}W_{0.98}O_3$.

The lower magnification SEM micrograph of the CsSr–MoW–HTB–PAN-1000 phase assemblage appeared relatively similar to that of the 800 °C sample, comprising of a large proportion of block-like crystallites of composition $Mo_{\sim 0.02}W_{\sim 0.98}O_3$. The number of rod-like crystallites observed in this sample was substantially higher than that observed for the 800 °C sample. Additionally, a significant proportion of fibrous crystallites were now observed in the interstitial regions between the MO_3-like crystallites (Fig. 8). Again, the full complement of Cs was observed to be distributed amongst the rod-like crystallites with the level of Na again equaling that of the Cs present. In all regions analysed, Sr was not observed in these phases indicating that the partitioning of Sr away from the Cs-HTB phase was directly linked to the calcination temperature. Strontium was found in the lower contrast interstitial regions which consist of interconnected fibers of general composition $A_{0.3}Mo_{0.2}W_{0.8}O_3$. The change in the average molybdenum content for these regions shows that the calcination temperature strongly affects the partitioning of molybdenum throughout the phase assemblage in a similar fashion to that of strontium.

In the sample heated to 1200 °C there was a lower proportion of the previously observed MO_3 block particles compared to that of the fibrous and ill-defined interstitial regions (Fig. 9). The typical composition of the MO_3 regions contained ~4–5% Mo was slightly higher than that observed for the 800 and 1000 °C samples at ~2% Mo. The fibrous crystallites of this phase assemblage again contained all the observable Cs and an approximately equal proportion of Na. However, the presence of Sr was observed in all such particles. All of the fibrous crystallites exhibited essentially the ideal $A_{0.3}MO_3$ composition for a HTB phase. Given that Cs was found at all temperatures in these HTB-like

Fig. 8. SEM micrograph of CsSr–MoW–HTB–PAN-1000. Spot EDS analyses were taken at the centre of the marks. 1 – $A_{0.3}Mo_{0.14}W_{0.86}O_3$; 2 – $A_{<0.03}Mo_{0.04}W_{0.96}O_3$; 3 – $A_{<0.01}Mo_{0.02}W_{0.98}O_3$; 4 – $Mo_{0.02}W_{0.98}O_3$; 5 – $A_{0.36}Mo_{0.22}W_{0.78}O_3$; 6 – $A_{0.35}Mo_{0.22}W_{0.78}O_3$; 7 – $A_{0.35-0.38}Mo_{0.02}W_{0.98}O_3$.

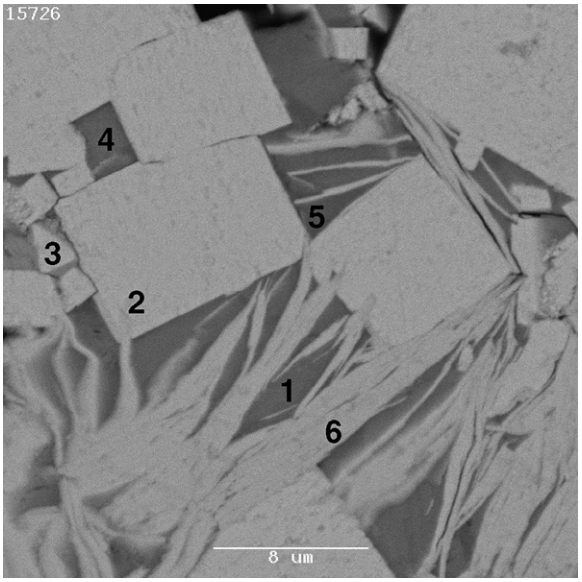

Fig. 9. SEM micrograph of CsSr–MoW–HTB–PAN-1200. Spot EDS analyses are taken at the center of the marks. 1 – $A_{0.37}Mo_{0.19}W_{0.81}O_3$; 2 – $A_{<0.03}Mo_{0.04}W_{0.96}O_3$; 3 – $A_{<0.04}Mo_{0.12}W_{0.88}O_3$; 4 – $A_{0.59}Mo_{0.65}W_{0.35}O_3$; 5 – $A_{0.65}Mo_{0.7}W_{0.3}O_3$; 6 – $A_{0.3}Mo_{0.18}W_{0.82}O_3$.

phases, we believe that this supports our earlier assertions that Cs^+ promotes the formation, or indeed, stabilises the HTB phase at higher temperatures. Sodium cations, and to a much lesser extent Sr^{2+}, appear to principally act as charge compensators. The largest difference upon heating to 1200 °C was the extensive partitioning of Mo into the lower contrast, interstitial regions between the fibrous crystallites. These regions displayed A:Mo:W ratios of 0.6:0.7:0.3 and as such it is unlikely that these regions correspond to HTB phases.

3.3. Durability testing – Modified PCT leaching

The leach resistances of the CsSr–MoW–HTB–PAN-x phase assemblages were investigated using a modified PCT test incorporating an increased liquid-to-solid ratio of 100 ml/g over 1, 4 and 7 day periods. The increased liquid-to-solid ratio was employed to avoid saturation of the leachate, and hence, depressed fractions of Cs and Sr leached, as well as to minimise the potential precipitation of less soluble leached elements, or solution species thereof.

As in part 1 of this series, samples of Cs-Hollandite ($Cs_{0.10}Ba_{1.0}Al_{2.1}Ti_{5.9}O_{16}$ with mean particle size of 100 μm) and Sr-Titanate ($SrTiO_3$ with mean particle size <5 μm) were included for comparison and bench-marking as they are the principle phases in synroc which are employed for cesium and strontium retention. Fractional elemental losses (Cs and Sr) and the corresponding leach rates for CsSr–MoW–HTB–PAN-x ($x = 600$, 800, 1000 and 1200) are given in Table 2.

The plots in Figs. 10 and 11 show the fraction of Cs and Sr, respectively, leached from CsSr–MoW–HTB–PAN-x samples as a function of time. Firstly, the fractional Cs loss from the CsSr–MoW–HTB–PAN-x ($x = 600$, 800 and 1200) samples at 1, 4 or 7 days were all found to lie below about 8×10^{-5} (rate = $<1.2 \times 10^{-4}$ g/m^2/day) which is far superior to the value of 1.43×10^{-3} obtained for Cs-Hollandite at 4 days (Fig. 4; ---; rate = 3.05×10^{-4} g/m^2/day). The 1000 °C variant exhibited a 3-fold higher fractional Cs loss between 1 and 4 days, and decreased to 2×10^{-5} at 7 days. This variation was completely reproducible (triplicate analysis) with the fractional Sr loss being also consistent, and so was not a product of variable sampling. Given that Cs partitioning in the 1000 °C variant was comparable to the other CsSr–MoW–HTB–PAN-x samples studied, the decrease in durability is somewhat puzzling. The SEM investigations discussed previously highlighted the apparent partitioning of Sr away from HTB phases containing Cs at this temperature but at this point it is unclear whether this is a contributing factor to this behavior. Additionally, the measured levels of framework elements in the

Table 2
Fraction of Cs^+ and Sr^{2+} leached and BET normalized rate (g/m^2/day) from modified PCT leach testing of CsSr–MoW–HTB–PAN-x ($x = 600$, 800, 1000 and 1200) for 1, 4 and 7 day periods

PCT	1 day				4 day				7 day			
	Cs		Sr		Cs		Sr		Cs		Sr	
x	f	g/m^2/day	f	g/m^2/day	f	g/m^2/day	F	g/m^2/day	f	g/m^2/day	f	g/m^2/day
600	5.60×10^{-5}	2.58×10^{-5}	2.95×10^{-3}	1.36×10^{-3}	6.92×10^{-5}	7.97×10^{-6}	2.96×10^{-3}	3.40×10^{-4}	2.32×10^{-5}	1.53×10^{-6}	4.77×10^{-3}	3.14×10^{-4}
800	7.96×10^{-5}	1.26×10^{-4}	2.35×10^{-3}	3.73×10^{-3}	2.94×10^{-5}	1.17×10^{-5}	3.46×10^{-3}	1.37×10^{-3}	6.12×10^{-5}	1.39×10^{-5}	2.92×10^{-3}	6.62×10^{-4}
1000	1.61×10^{-4}	2.02×10^{-4}	5.81×10^{-3}	7.29×10^{-3}	1.67×10^{-4}	5.30×10^{-5}	8.36×10^{-3}	2.61×10^{-3}	2.50×10^{-5}	4.47×10^{-6}	5.19×10^{-3}	9.29×10^{-4}
1200	9.99×10^{-7}	1.19×10^{-6}	2.39×10^{-3}	2.85×10^{-3}	2.24×10^{-5}	6.57×10^{-6}	2.47×10^{-3}	7.37×10^{-54}	1.06×10^{-6}	1.81×10^{-7}	8.54×10^{-4}	1.45×10^{-4}
Hollandite	–	–	–	–	1.43×10^{-3}	3.05×10^{-4}	–	–				
$SrTiO_3$							3.10×10^{-3}	2.63×10^{-4}				

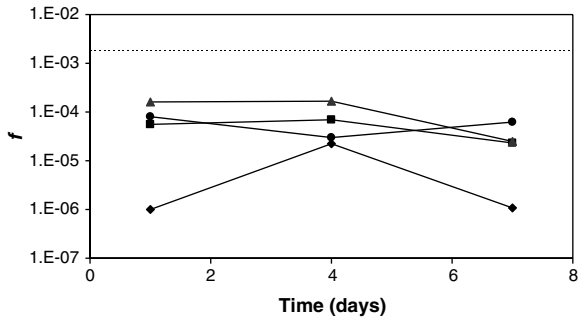

Fig. 10. Fractional Cs^+ loss (f) from CsSr–MoW–HTB–PAN-x ($x = 600$, 800, 1000 and 1200) at 1, 4 and 7 day periods. ■ – 600 °C, ▲ – 800 °C, ● – 1000 °C, ◆ – 1200 °C. Fractional Cs loss from Cs-hollandite (- - -).

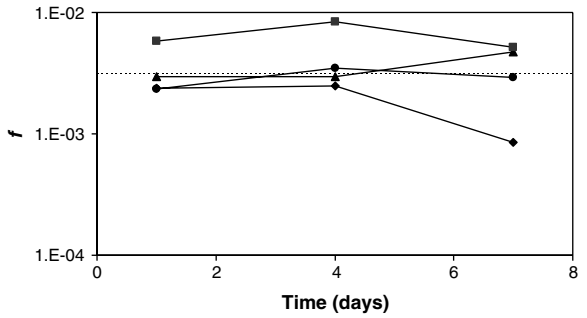

Fig. 11. Fraction Sr^{2+} loss (f) from CsSr–MoW–HTB–PAN-x ($x = 600$, 800, 1000 and 1200 °C) at 1, 4 and 7 day periods. ■ – 600 °C, ▲ – 800 °C, ● – 1000 °C, ◆ – 1200 °C. Fractional Sr loss from Sr-titanate ($SrTiO_3$) reference (- - -).

leachate were comparable or lower than that observed for the 600, 800 and 1200 °C samples, and hence, dissolution of an as yet unidentified Cs-containing phase can be discounted. Despite the higher fractional Cs loss for this sample, these results demonstrate the ability of the HTB phase to adequately retain Cs regardless of the higher Na concentration than that studied previously, and thermal history.

The fractional Sr loss from the CsSr–MoW–HTB–PAN-x samples over the 1–4 day period (Fig. 11) was relatively consistent at about 3×10^{-3} and compared favorably with the performance of the $SrTiO_3$ reference phase ($f = 3.1\times10^{-3}$; rate = 2.63×10^{-4} g/m^2/day). After 7 days, an overall decrease in the fraction leached for the 1200 °C sample was observed with the 600 °C sample exhibiting a 30% increase. As observed in the case of Cs leachability, the 1000 °C sample consistently exhibited decreased durability. This sample displayed a fraction of Sr leached almost twice that of the other CsSr–MoW–HTB–PAN-x samples at 1 day (~6 ×

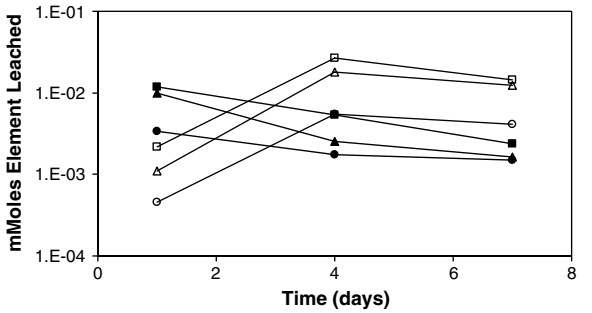

Fig. 12. Degree of matrix element dissolution (mmol) for CsSr–MoW–HTB–PAN-x ($x = 600$ and 800) at 1, 4 and 7 day periods during PCT leach testing. ▲ – Mo 600 °C, ● – W 600 °C, ■ – Na 600 °C, △ – Mo 800 °C, ○ – W 800 °C, □ – Na 800 °C.

10^{-3}), increasing to almost three times ($f = \sim 8.5 \times 10^{-3}$; rate $= 2.6 \times 10^{-3}$ g/m^2/day) at 4 days. As discussed during the presentation of the Cs leach results for the 1000 °C sample, it is difficult to definitively ascribe the decreased durability of the 1000 °C sample to the presence of HTB phases which do not contain both Cs^+ and Sr^{2+}.

Along with the fraction of Cs^+ and Sr^{2+} leached from the CsSr–MoW–HTB–PAN-x samples using the modified PCT protocol, the levels of the matrix elements Mo and W were monitored, as well as the level of Na present in the final leachates (Figs. 12 and 13). For the CsSr–MoW–HTB–PAN heated to 600 and 800 °C there was a strong correlation between the level of all three framework elements in the resultant leachates from 1 to 7 days of leaching. This is inline with the measured fractions of Cs and Sr leached and associated leach rates for these samples which were also comparable over the leaching periods studied here. Furthermore, given that Sr was found to partition away from Cs on heating to

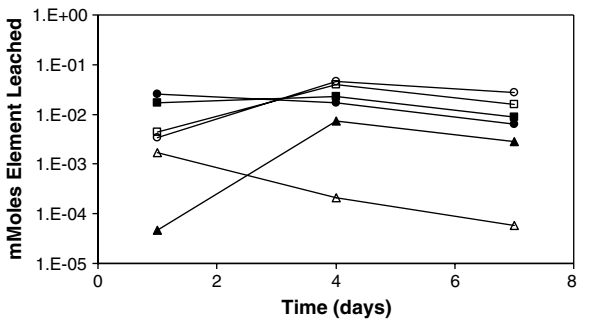

Fig. 13. Degree of matrix element dissolution (mmol) for CsSr–MoW–HTB–PAN-x ($x = 1000$ and 1200) at 1, 4 and 7 day periods during PCT leach testing. ▲ – Mo 1000 °C, ● – W 1000 °C, ■ – Na 1000 °C, △ – Mo 1200 °C, ○ – W 1200 °C, □ – Na 1200 °C.

800 °C to a HTB phase containing just sodium cations, the favourable leach characteristics for Sr appear to depend more on the host HTB framework than the high content of Na in this phase. This is an extremely positive feature for the MoW–HTB–PAN composite system, as in a practical scenario the exhausted composite is likely to contain more sodium than radiogenic cesium or strontium.

Heating of the CsSr–MoW–HTB–PAN at 1000 °C saw a significantly lower level of 1 day fractional Mo loss than for W and Na. For leaching periods of 4 and 7 days the level of Mo was consistent with W and Na as was observed in the case of the CsSr–MoW–HTB–PAN-x ($x = 600$ and 800) samples. It is worth noting that this is the first temperature where there was a significant partitioning of Mo towards what appeared to be a HTB phase, i.e., ~20% Mo and that higher leached fractions of Sr were consistently observed between 1 and 7 days. It would be reasonable to assume that a lower level of matrix dissolution should lead to a depressed Sr fraction leached given the observed partitioning of Sr towards this Mo-rich phase. However, this assessment assumes that matrix dissolution is the rate limiting factor for cation leaching. This does not appear to be the case in this instance and another mechanism appears to be at play. As shown previously, incorporation of low to medium levels of Mo into the HTB framework introduces significant disorder to the HTB framework, and this in-turn plays a critical role in determining the selectivity of the phase for Cs and Sr. It is our hypothesis that the Mo-rich HTB framework experiences sufficient disruption through increased molybdenum incorporation so that the Sr^{2+} siting within the phase is significantly affected. This in turn leads to decreased durability than that of the HTB phase with low levels (2–5% total metal content) of molybdenum incorporation, thereby giving rise to the higher fraction of Sr leached from the sample heated to 1000 °C.

With heating to 1200 °C, the degree of molybdenum partitioning into a HTB phase was seen to decrease and instead favoured formation of a phase exhibiting A:Mo:W ratios of 0.6:0.7:0.3. Along with the fractions of Cs and Sr leached from this sample, the observed levels of molybdenum dissolution between 1 and 7 days were amongst the lowest levels observed for any of the CsSr–MoW–HTB–PAN-x samples. Although the exact structure of the cation- and Mo-rich phases are unknown at this stage it is apparent from our experimental data that these are at least in part responsible for the superior

durability with respect to the Cs-Hollandite and $SrTiO_3$ reference phases.

3.4. Durability testing – 0.10 M HNO_3 leaching

In our previous investigations of the durability of Cs- and Sr-containing HTB phases we have employed dilute nitric acid solutions in place of Millipore water during modified PCT leach tests so as to significantly test the ability of the concerned materials to retain adsorbed Cs and Sr. Moreover, the lowering of pH through the radiolysis of water and the consequences that this has on the safety of wasteforms and spent fuel in a repository situation was raised long ago as a serious concern [9,10]. The leaching data for CsSr–MoW–HTB–PAN samples heated between 600 and 1200 °C in 0.1 M HNO_3 for 4 days is presented in Fig. 14 and also Table 3. As employed previously, both Cs-Hollandite and $SrTiO_3$ were included for comparison, with comparable tests also conducted on a MoW–HTB adsorbent which had been fully exchanged with Cs and Sr (sat. 900). The latter material is that which was the subject of investigations reported in part 1 of this series and it was anticipated that this might provide further insight into the effect of cation loading in the MoW–HTB-based wasteforms.

For the two reference phases the results in Fig. 14 show quite clearly that their durability under acidic conditions was extremely poor with about 20% of Cs leached and complete removal of Sr. For all of the tungstate phase assemblages, the durability with respect to Cs was significantly superior with the lowest fraction leached observed for the CsSr–MoW–HTB–PAN heated to 1000 °C. In fact, heating the loaded composite between 800 and 1200 °C was sufficient to decrease the fraction of Cs leached to almost two orders of magnitude better than the Cs-Hollandite reference phase. With respect to Sr, the minimum fractional release was observed for the CsSr–MoW–HTB–PAN heated to 800 °C and was in stark contrast to the sat. 900 sample which was unable to retain essentially any Sr under such conditions. The leachability of the sat. 900 sample was in accord with the behavior described during part 1 of this series, and we ascribe the differences between the tungstate phase assemblages to the different partitioning behavior of Sr^{2+} in each system. For the sat. 900 sample, the apparent cubic phase containing the full complement of the Sr is not particularly leach resistant under these acidic conditions, although at intermediate pH values the leach resistance improves considerably (refer to part 1). Furthermore, the ability of Sr to partition into the more durable HTB phases in the CsSr–MoW–HTB–PAN-x samples when the total Cs content is low allows favorable leach resistance under either acidic or neutral conditions.

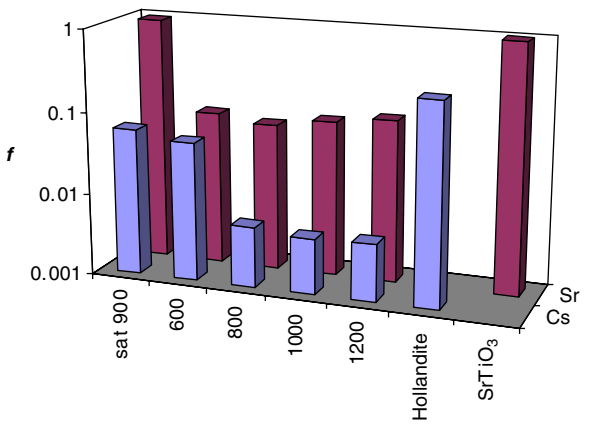

Fig. 14. Comparison of Cs and Sr fractional releases (f) from various tungstate-based ceramic wasteforms and reference phases using 0.1 M HNO_3 at 150 °C for 4 days.

Table 3
Fractional releases of Cs and Sr and BET normalised rate (g/m^2/day) from leach testing of CsSr–MoW–HTB–PAN-x ($x = 600$, 800, 1000 and 1200) using 0.1 M HNO_3 at 150 °C for 4 days

HNO_3	4 day			
	Cs		Sr	
x	f	g/m^2/day	f	g/m^2/day
Sat. 900	6.1×10^{-2}	2.7×10^{-2}	9.5×10^{-1}	–
600	4.88×10^{-2}	5.61×10^{-3}	7.51×10^{-2}	8.64×10^{-3}
800	5.44×10^{-3}	2.16×10^{-3}	6.19×10^{-2}	2.46×10^{-2}
1000	4.74×10^{-3}	1.48×10^{-3}	7.84×10^{-2}	2.46×10^{-2}
1200	5.01×10^{-3}	1.49×10^{-3}	9.43×10^{-2}	2.81×10^{-2}
Hollandite	2.74×10^{-1}	1.38×10^{-2}	–	–
$SrTiO_3$	–	–	1.006	1.32×10^{-1}

4. Discussion

The thermal treatment of the CsSr–MoW–HTB–PAN system partially exchanged with Cs^+ and Sr^{2+} that was examined here appears to afford results which are in many aspects consistent with those of the Cs^+- and Sr^{2+}-saturated MoW–HTB fine grained powders examined in part 1 of this series. Here the air-dried CsSr–MoW–HTB–PAN materials have been shown unequivocally by ^{133}Cs solid state NMR to be multiphasic even prior to heating. Heating at 600 °C generated a similar NMR spectrum to the unheated sample but allowed the distinct mor-

phologies and compositions to be observed in the cross-sectional SEM images of the resulting tungstate ceramic phase assemblage that derives from this unheated material. XRD suggests that HTB–WO_3 intergrowth structures and CsSr-containing MoW–HTB phases form part of this phase assemblage.

Thermal treatment of both A–MoW–HTB powders and A–MoW–HTB–PAN composite materials to temperatures above about 500 °C gave rise to the crystallization of WO_3 and some redistribution of Cs. One particular difference is that the saturated fine-grained powders which contained a higher Cs and Sr content displayed fractional Cs losses that appear somewhat greater than that observed in the present study for materials that have much lower Cs and Sr loadings. More specifically, in the saturated powders of part 1 we have obtained 4-day fractional losses in water of the order of 1×10^{-2} for both Cs–MoW–HTB and Sr–MoW–HTB phases heated at 600 °C whereas for the CsSr–MoW–HTB–PAN-600 sample examined here we have obtained values of about 1×10^{-4} and 1×10^{-2}, respectively for Cs and Sr losses. Whether this variation is exclusively a consequence of the higher loadings or is due to batch variability and/or differences in the processing conditions is difficult to tell. Discrete Sr-containing molybdenum tungsten oxide phases with compositions such as $Sr_{0.6}Mo_{0.3}W_{0.5}O_3$ are able to crystallize in Sr–MoW–HTB samples thermally treated to 1000 °C whereas no such phases are ever detected in the CsSr–MoW–HTB–PAN system. Certainly, neither the reducing conditions imparted by the presence of large concentrations of organics or the presence of large concentrations of Na seriously affects the phase chemistry and the resultant performance of the tungstate ceramics produced.

In comparison to our research presented in part 1 of this series, the favorable leach characteristics of the present materials under acidic or neutral pH is certainly the result of partitioning of *both* Cs and Sr into HTB-like phases. We believe that this is due to the low initial level of Cs in the MoW–HTB–PAN composite being insufficient to saturate the HTB phases formed on heating between 600 and 1200 °C, and so enabling Sr to partition in a similar manner to that of Cs.

5. Conclusions

Tungstate phase assemblages prepared from the simple thermal treatment of Cs- and Sr-containing MoW–HTB–PAN composite adsorbent display excellent leach resistance using a modified PCT protocol (unwashed powder; $V/m = 100$ ml/g) employing either Millipore water at 90 °C, or 0.1 M HNO_3 at 150 °C. These performances match or better those of the saturated powdered phases and are at least as good as any of the titanate reference materials used for comparison.

The combination of the ability to produce durable, leach resistant tungstate nuclear wasteform ceramics from simple heating in air, along with the significant waste volume reduction potential via pretreatment with the MoW–HTB–PAN composite adsorbent, makes this approach highly attractive for the processing of acidic waste streams in which the majority of activity results from radiogenic Cs and Sr.

The production of reasonably well consolidated pellets on calcination of CsSr–MoW–HTB–PAN in air is potentially advantageous since it eliminates the hazards associated with the manipulation of powdered materials.

Other aspects that need to be treated as far as the tungstate wasteform system is concerned involves the tolerance to the presence of other metallic and fission product elements. Issues pertaining to these aspects will be treated in part 3 of this series.

Acknowledgements

The authors are grateful to Patricia Gadd of ANSTO for providing the XRF analyses and to Dr K. Pike of ANSTO for assistance with the acquisition of the high field MAS data.

References

[1] V. Luca, C.S. Griffith, H. Chronis, J. Widjaja, H. Li, N. Scales, Mater. Res. Soc. Symp. Proc. 807 (2004) 309.
[2] C.S. Griffith, V. Luca, Chem. Mater. 16 (2004) 4992.
[3] V. Luca, E. Drabarek, C.S. Griffith, H. Chronis, J. Foy, Mater. Res. Soc. Symp. Proc. 807 (2004) 303.
[4] F. Sebesta, NATO Sci. Ser., Ser. E: Appl. Sci. 362 (1999) 473.
[5] F. Sebesta, V. Stefula, J. Radioanal. Nucl. Chem. 140 (1990) 15.
[6] C.S. Griffith, V. Luca, P. Yee, F. Sebesta, Sep. Sci. Technol. 40 (2005) 1781.
[7] K.P. Reis, A. Ramanan, M.S. Whittingham, J. Solid State Chem. 96 (1992) 31.
[8] H.-T. Kim, C.-H. Lee, Y.-G. Shul, J.-K. Moon, E.-H. Lee, Sep. Sci. Technol. 38 (2003) 695.
[9] A. Barkatt, A. Barkatt, W. Sousanpour, Nucl. Technol. 60 (1983) 218.
[10] G.L. McVay, W.J. Weber, L.R. Pederson, Nucl. Chem. Waste Manage. 2 (1981) 103.